Ultrasound of the Elbow

4

Janeth Yinh, Amy Evangelisto, and Minna J. Kohler

Key Points

- Ultrasound can be helpful in evaluating commonly encountered rheumatologic conditions involving the elbow, such as rheumatoid arthritis, psoriatic arthritis, and crystal-induced arthritis.
- Ultrasound investigation of the tendons can characterize structural abnormalities in the tendon to help differentiate from inflammatory vs. mechanical conditions.
- Ultrasound aids in the characterization of nodules in the elbow (e.g., heterogeneous echogenicity in gouty tophi vs. homogeneous echogenicity with hypoechoic center seen in rheumatoid nodules).
- Dynamic ultrasound of the elbow can enhance visualization of sonographic pathology affecting structures in motion (e.g., ulnar nerve subluxation, snapping tendon, confirmation of intra-articular loose bodies within the joint, ligament, and tendon disruption).

J. Yinh (✉) · M. J. Kohler
Division of Rheumatology, Allergy, and Immunology, Department of Medicine, Massachusetts General Hospital, Harvard Medical School, Boston, MA, USA
e-mail: janeth.yinh@mgh.harvard.edu; mkohler@mgh.harvard.edu

A. Evangelisto
Arthritis, Rheumatic and Back Disease Associates, Voorhees, NJ, USA

M. J. Kohler (ed.), *Musculoskeletal Ultrasound in Rheumatology Review*,
https://doi.org/10.1007/978-3-030-73555-5_4

Introduction

Ultrasound of the elbow is useful in evaluating the elbow for commonly encountered pathology in rheumatology and other musculoskeletal clinics. The articulations and synovium of the elbow joint and surrounding soft tissue structures such as tendons, ligaments, muscles, nerves, and bursa are easy to examine using musculoskeletal ultrasound. Synovitis, tendinitis, enthesitis, effusions, tendon, and ligament pathology can be characterized when physical exam findings are equivocal.

Elbow ultrasound of the joint recess can help distinguish the presence of synovial tissue vs. fluid and increase the likelihood of a successful aspiration. Evaluation of tendons with elbow sonography may complement in visualizing the extent of tendon derangement and on occasions help provide characteristic features that may help distinguish mechanical vs. inflammatory pathology.

Ultrasound Examination Technique

The ideal position to begin scanning the elbow is with the patient seated or supine with the elbow extended and the hand supinated. Positioning a pillow to support the extremity stabilizes the elbow in position to avoid motion artifact and provides comfort for the patient. In cases where elbow pathology does not allow full extension of the elbow, a generous amount of gel may assist in providing full contact of the probe for better visualization of anterior structures viewed longitudinally. Positioning the arm abducted with the elbow extended or semiflexed facilitates scanning of the medial elbow.

The use of a high-frequency linear array probe ranging from 5 to 12 MHz seeking the highest frequency that permits the best penetration of the structures of interest is recommended. The choice of probe and ideal frequency may be affected by the patient's body habitus. Adjustments in the depth can then be applied for more conspicuous visualization of deeper structures.

An organized scanning protocol (see Table 4.1) can visualize normal anatomy and allow the sonographer to focus on particular pathology related to the regional structures. Figure 4.1 provides a useful guide of the relevant bony landmarks of the elbow to keep in mind when scanning the elbow. Upon identifying the view or structure of interest, it is important to slide the transducer from side to side as well as proximally and distally to capture boundaries of structures and not miss any possible abnormalities.

Anterior Elbow

Scan of the anterior elbow can evaluate the humeroradial and humeroulnar joints with their corresponding radial and coronoid fossa: the articular cartilage, brachialis muscle, biceps brachii tendon, and median nerve.

Table 4.1 Elbow scanning protocol: structures of interest with indications and key features

View	Structures of interest	Indications/key features
Anterior	Anterior elbow recess (humeroradial/humeroulnar) Brachialis muscle Median nerve Biceps muscle/tendon insertion Femoral cartilage	Synovitis, effusion, or erosions, loose bodies *(displaceable with dynamic evaluation)* Bicipitoradial bursitis Median nerve entrapment Distal biceps tendon tear Osteoarthritis: cartilage degeneration. Crystal deposition: gout *(deposition overlying cartilage)* vs. pseudogout *(deposition within cartilage)*
Lateral	Common extensor tendon Lateral collateral ligament complex Annular recess (radial head)	Tendinosis, tear, calcification, enthesitis[a] *(abnormal tendon features)* Ligament laxity or partial or complete tear Synovitis, effusion, or erosions
Medial	Common flexor tendon Medial olecranon joint Ulnar collateral ligament (UCL)	Tendinosis, tear, calcification, enthesitis[a] *(abnormal tendon features)* Synovitis, effusion, or erosions Ligament laxity or partial or complete tear of the anterior band of the UCL
Posterior	Triceps tendon Posterior joint recess Olecranon bursa Ulnar nerve	Tendinosis, tear, calcification, enthesitis[a] *(abnormal tendon features)* Synovitis, effusion, or erosions, loose bodies *(displaceable with dynamic evaluation)* Bursitis (hypoechoic thickening or anechoic compressible fluid) or nodules Thickening or hypoechogenicity of the ulnar nerve, entrapment, or subluxation *(dynamic maneuvers may confirm subluxation/snapping triceps syndrome)*

[a]Abnormal tendon features: *tendinosis*, echotexture, or tendon contour changes (e.g., loss of fibrillar pattern, hypoechogenicity, thickening). *Tear*: anechoic defect in two orthogonal planes; dynamic views of extensor tendon may confirm tear. Tear may have surrounding fluid or power Doppler signal. *Enthesitis:* color power Doppler signal may be noted within tendon or bony entheses. Cortical irregularities can be noted in chronic tendinitis or inflammatory spondyloarthropathy

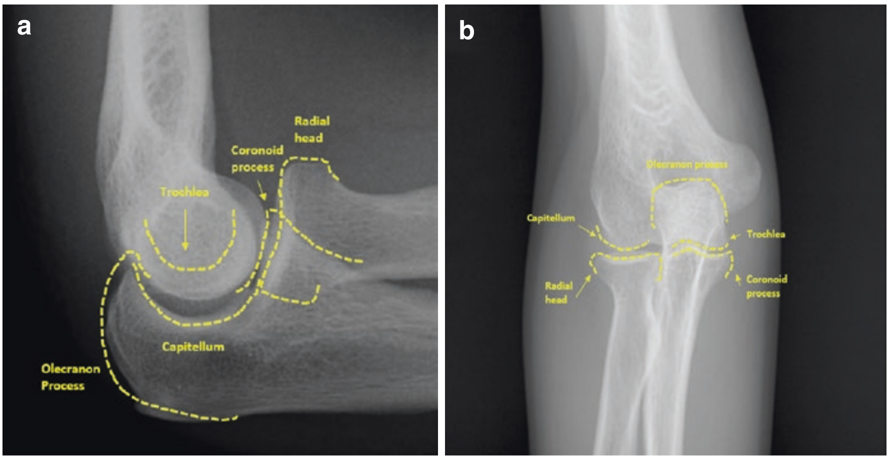

Fig. 4.1 Relevant bony landmarks of the elbow. (**a**) Lateral view. (**b**) Posterior view

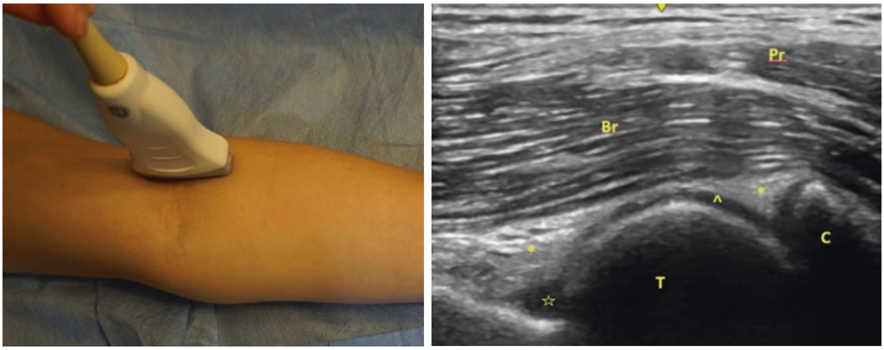

Fig. 4.2 Anterior longitudinal view of the humeroulnar or ulnotrochlear joint: probe positioning with ultrasound view. Trochlea (T), coronoid (C), brachialis muscle (Br), pronator teres muscle (Pr), fat pad (*), coronoid fossa (star), articular cartilage (^)

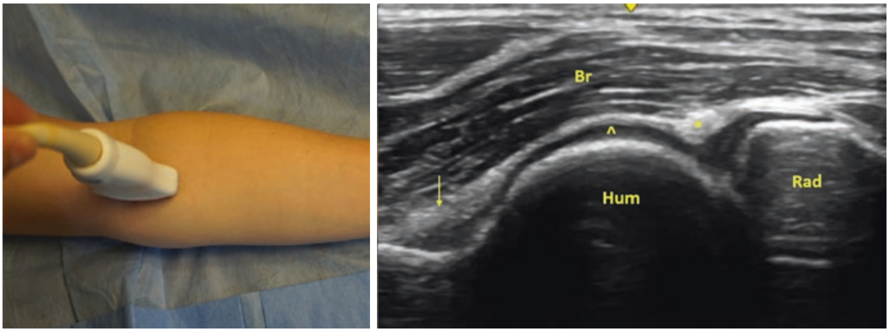

Fig. 4.3 Anterior longitudinal humeroradial or radiocapitellar joint: brachioradialis muscle (Br), humerus (Hum), radial head (Rad), coronoid fossa (arrow), cartilage (^), fat pad (*)

To evaluate the longitudinal view of the humeroulnar or ulnotrochlear joint, the probe is placed perpendicular to the elbow crease over the extended elbow medially. The bony landmarks to identify include the trochlea of the medial humerus articulating with the "peaked or triangular" coronoid process of the ulna (Fig. 4.2). Scanning the humeroulnar joint proximally will evaluate the coronoid fossa that is occupied by a triangular hyperechoic fat pad. Performing a heel-toe maneuver of the probe can assist in enhancing the distal bony contour of the coronoid process that angles sharply away from the joint space appearing as a "mountain peak." The brachialis muscle overlying the joint can be scanned distally to its insertion to the tuberosity of the radius.

Sweeping the probe laterally will display the lateral capitellum of the humerus articulating with the boxy-appearing radial head that conforms the humeroradial or radiocapitellar joint (Fig. 4.3). Physiologic hyperechoic fat will also overlie the cartilage at this site creating a "seagull" appearance over the joint cleft that is appreciated at the humeroulnar joint. In the presence of effusion or synovitis, this hyperechoic "seagull"-appearing fat pad may be distorted and shifted anteriorly [1].

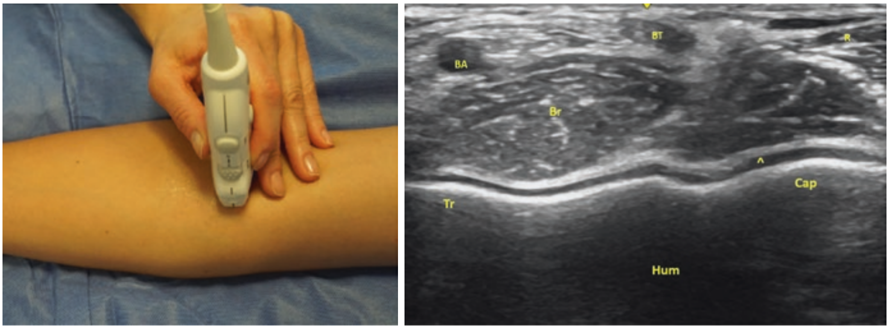

Fig. 4.4 Anterior transverse view. Humerus (Hum), trochlear portion of humerus (Tr), capitellar portion of humerus (Cap), brachialis muscle (Br), bicipital tendon (BT), brachial artery (BA), radial nerve (R), articular cartilage (^). Left is medial and right is lateral

Scanning the humeroradial joint proximally will identify the radial fossa and more distally the annular recess to evaluate for the presence of fluid. It is useful to dynamically assess the joint with supination and pronation to assist in the detection of loose bodies as well as identification of smaller fluid collections. The brachioradialis muscle is the muscle that runs over the humeroradial joint. Slightly distal, directly on top of the radial shaft, the supinator muscle can be visualized.

The probe can then be rotated 90 degrees almost parallel to the elbow crease with slight movements proximally and distally to evaluate the anterior transverse view of the elbow joint (Fig. 4.4). At this level, the distal humerus has a distinctive wavy appearance with a thick anechoic cartilage appearing similar to the surface of a "clam shell." One must be aware to avoid confusing this anechoic hyaline cartilage lying directly over the articulating bone for an effusion that is also anechoic at the same location. The echogenic joint capsule will lie directly on the hyaline cartilage of the distal humerus, whereas separation of the structures will be seen in the presence of an effusion or synovitis. Note the trochlear portion of the humerus on the left and the capitellum of the humerus laterally on the right. Sweeping the probe cranially will assess the radial and coronoid fossa that can identify fluid or abnormal synovium extending proximally. The brachialis muscle is located centrally over the humerus, the extensor carpi radialis and brachioradialis muscle lying superficially on the lateral aspect. The median nerve medially and radial nerve laterally can be seen between the muscles.

The anterior transverse windows also evaluate the biceps brachii tendon that lies lateral to the brachial artery and superficial to the brachialis muscle. The bicipitoradial and interosseous bursa which are virtual cavities that are only identified in cases of pathology can be evaluated through the anterior transverse elbow view. The integrity of the tendon can be assessed in short axis tracking its proximal and distal portions to the insertion to evaluate for tears of the tendon. The biceps brachii tendon can also be evaluated in long axis superficial to the brachialis muscle as a hyperechoic fibrillar structure located lateral to the brachial artery. As the biceps brachii tendon courses over the elbow joint, it takes a steep and slight oblique course

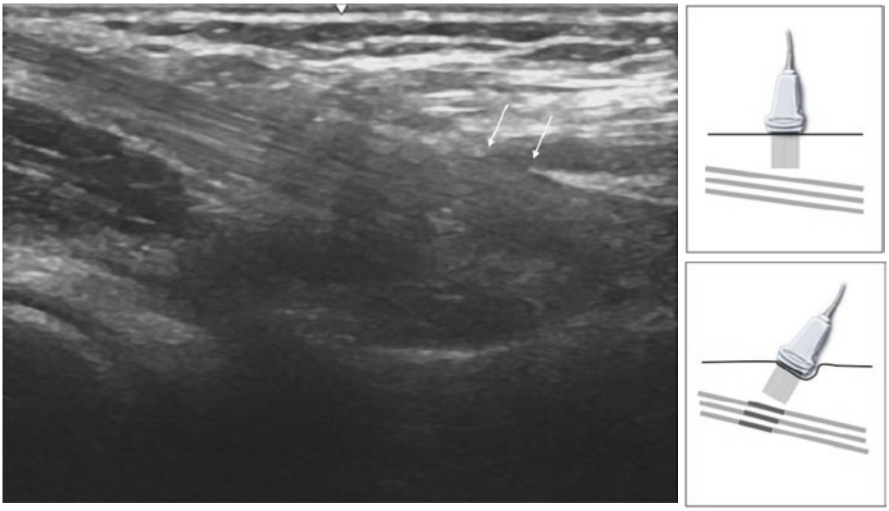

Fig. 4.5 Longitudinal view of the biceps tendon. Right side demonstrates "heel-toe" probe positioning maneuver applying increased pressure distally to overcome tendon anisotropy

making its appearance become more hypoechoic as it inserts onto the radial tuberosity. This hypoechoic effect of the tendon from anisotropy can be reduced by applying a heel-toe maneuver or adjusting the elbow position with mild flexion or extension to obtain a more conspicuous view of the distal tendon (Fig. 4.5). The use of beam steering function (allows a point on an image to be insonated from multiple angles from a single probe and a single position of the probe) available in some ultrasound machines may also improve the visibility of the tendon. Dynamic assessment with supination and pronation can enhance evaluation of the distal fibers that will disappear with supination [2].

Lateral Elbow

The lateral elbow is evaluated with the elbow flexed and the arm internally rotated. The common extensor tendon can be visualized placing the proximal probe over the bony prominence of the lateral epicondyle parallel to the tendon (Fig. 4.6). Assessment of the common extensor tendon integrity, width, echogenicity, presence of hyperemia, and bony irregularities at its bony attachment and distal evaluation of the myotendinous junction are among the features included in a comprehensive tendon evaluation. It is recommended to evaluate the most anterior portion of the tendon where abnormalities can be frequently encountered. The radial collateral ligament is viewed as a thin hyperechoic fibrillar structure lying deep to the extensor tendon connecting the humerus and radius. Distinction of the radial collateral ligament fibers from the common extensor tendon can be performed by following its course that extends distally to the radial head blending with the annular ligament fibers. In contrast, the common extensor tendon has a different course that is seen

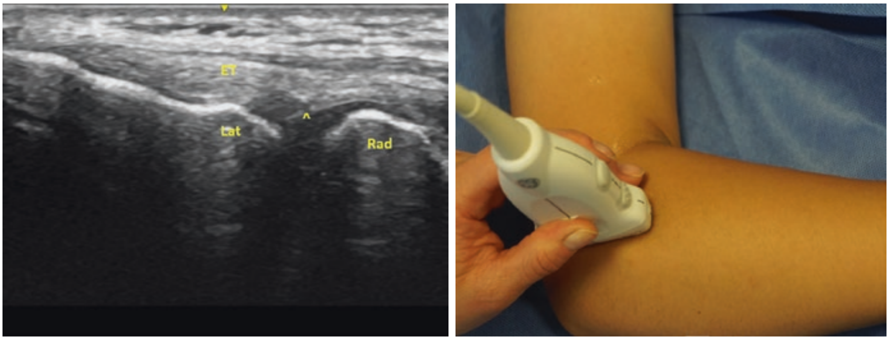

Fig. 4.6 Lateral longitudinal view. Lateral epicondyle (Lat), radial head (Rad), extensor tendon (ET), radial annular ligament (^)

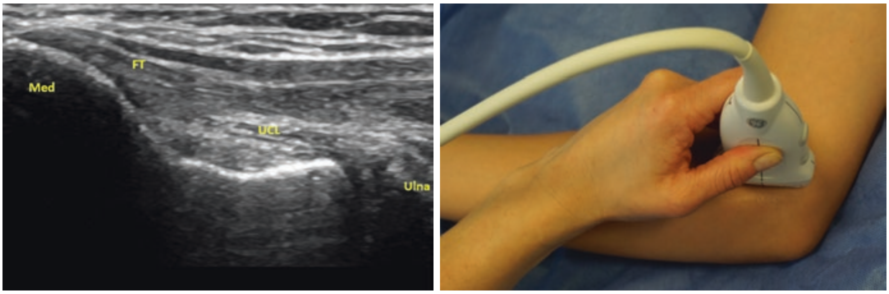

Fig. 4.7 Medial longitudinal view. Medial epicondyle (Med), ulna, flexor tendon (FT), ulnar collateral ligament (UCL)

superficially as a thicker fibrillar structure that extends distally to become muscle. The lateral radiocapitellar joint cleft is occupied by a triangular meniscus like synovial fold termed synovial fringe or posterolateral plica which may be symptomatic and misdiagnosed as lateral epicondylitis. At the radial neck, the annular recess is collapsed and poorly visualized in normal circumstances but will appear distended when occupied by synovium or fluid. The deep and superficial branches of the radial nerve can be identified transversely as a round hypoechoic structure between the fascial planes of the brachioradialis and brachialis anteriorly.

Medial Elbow

Scanning the medial elbow is best performed with the elbow extended or slightly flexed and the arm abducted in full supination. The probe is positioned in long axis with the proximal portion of the probe over the medial epicondyle (Fig. 4.7). The characteristic sloped appearance of the medial epicondyle can be easily identified as well as the superficial common flexor tendon overlying the anterior bundle of the ulnar collateral ligament. Evaluation of the same tendon features described above for the common extensor tendon should be assessed for the common flexor tendon.

The medial joint line between the humerus and the ulna is located distally deep to the ulnar collateral ligament. The ulnar collateral ligament is constituted by three components; the anterior band is functionally the most important and best visualized through ultrasound. The anterior band of the ulnar collateral ligament is seen as a compact hyperechoic fibrillar structure deep to the common flexor tendon that can be identified slightly shifting the probe off plane of the tendon to trace its attachment from the medial epicondyle of the humerus to the proximal ulna. Dynamic valgus stress with the elbow slightly flexed to disengage the olecranon from the olecranon fossa can aid in evaluating for injury of the ulnar collateral ligament [3].

Posterior Elbow

Positioning the arm with 90-degree flexion with the hand placed on the patients hip or a table will allow evaluation of the posterior elbow. The probe is placed proximal to the elbow in longitudinal plane with the tip of the probe supported over the olecranon process (Fig. 4.8). The superficial hyperechoic fibrillar triceps tendon overlying the olecranon fossa is evaluated for swelling, disruption, Doppler signal, calcifications, or bony irregularities at its insertion onto the olecranon. The bony contours of the olecranon, the joint cleft, and the pronounced concavity of the olecranon fossa can be clearly identified lying deep to the triceps muscle and tendon. The olecranon fossa is normally occupied by a hyperechoic posterior fat pad that is noted to be displaced superficially in the presence of an effusion. Dynamic flexion and extension can enhance evaluation of fluid or loose bodies at this site. Turning the probe 90 degrees to the triceps will image the transverse view of the olecranon recess (Fig. 4.9). Evaluation of the olecranon bursa that is only seen in abnormal conditions is best performed with the arm extended having caution to apply light pressure of the probe to avoid displacement of pathologic bursal fluid.

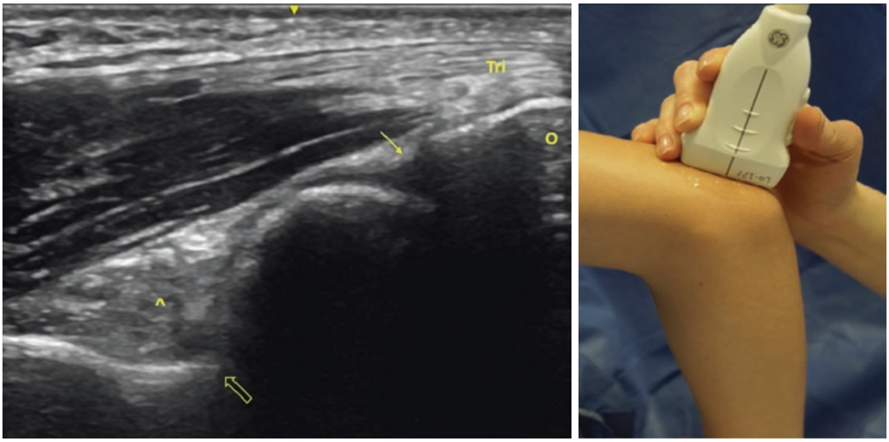

Fig. 4.8 Posterior longitudinal view. Olecranon process (O), triceps tendon (Tri), joint cleft (arrow), olecranon fossa (open arrow), fat pad (^)

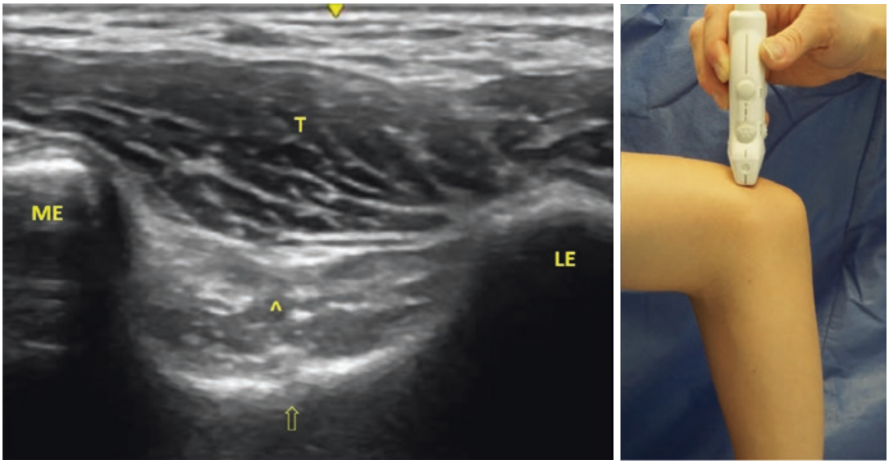

Fig. 4.9 Posterior transverse view. Triceps tendon (T), medial epicondyle of the humerus (ME), lateral epicondyle of the humerus (LE), olecranon fossa (open arrow), fat pad (^)

Fig. 4.10 Transverse view of the cubital tunnel. Medial epicondyle of the humerus (ME), ulnar nerve (arrow), medial joint cleft (^)

The probe can later be redirected bridging one end on the olecranon process and the other end at the medial epicondyle with the elbow turned outward to evaluate the cubital tunnel region. The ulnar nerve is visible as a speckled or honeycomb oval structure in close proximity to the medial epicondyle that can be evaluated for increased surface area indicative of swelling. Superficial to the ulnar nerve is the cubital tunnel retinaculum (or Osborne fascia) that is typically not seen in normal state. Dynamic assessment of the cubital tunnel in transverse view with elbow flexion and extension can reveal the presence of a subluxing ulnar nerve or a snapping triceps over the apex of the medial epicondyle (Fig. 4.10). Applying firm pressure with the transducer should be avoided as this may prevent displacement of the ulnar nerve from the ulnar tunnel. The examiner should also be cautious to evaluate for any space-occupying lesion within the cubital tunnel including bone spurs, ganglion cysts, effusion, or synovium that may compress or displace the ulnar nerve. Comparison with the asymptomatic side at the same level may also be utilized as an indicator of ulnar nerve swelling. Long axis of the ulnar nerve is performed by rotating the probe 90 degrees parallel to its tract which can reveal areas of nerve compression.

Rheumatologic Elbow Pathology

Synovial Pathology

Ultrasound is extremely useful for the detection of synovitis or effusion at the elbow where it has demonstrated to be more sensitive than physical exam and radiography in detecting effusions [4, 5]. Ultrasound evaluation of the elbow to identify synovial proliferation or effusion can be evaluated at various sites including the coronoid or radial fossa anteriorly, the annular joint recess laterally, and the medial joint cleft and the coronoid fossa posteriorly. Figures 4.11, 4.12, 4.13, 4.14, and 4.15 include examples of synovitis or effusion at each one of these sites. In these examples, it can

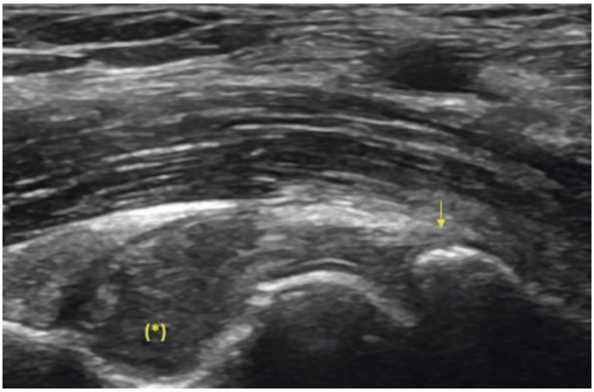

Fig. 4.11 Anterior longitudinal view demonstrating synovitis of the ulnotrochlear joint: coronoid fossa (*). Note the peak-like appearance of the ulna (arrow) to identify medial positioning of the probe

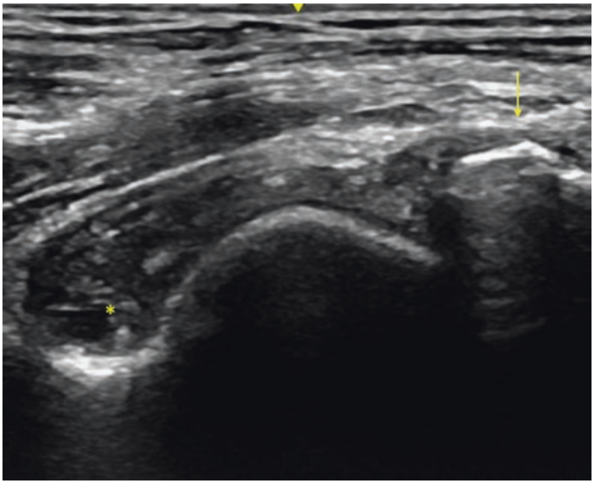

Fig. 4.12 Anterior longitudinal view of synovitis of the radiocapitellar joint: radial fossa (*). Note the "boxy appearance" of the radial head (arrow) to identify lateral positioning of the probe

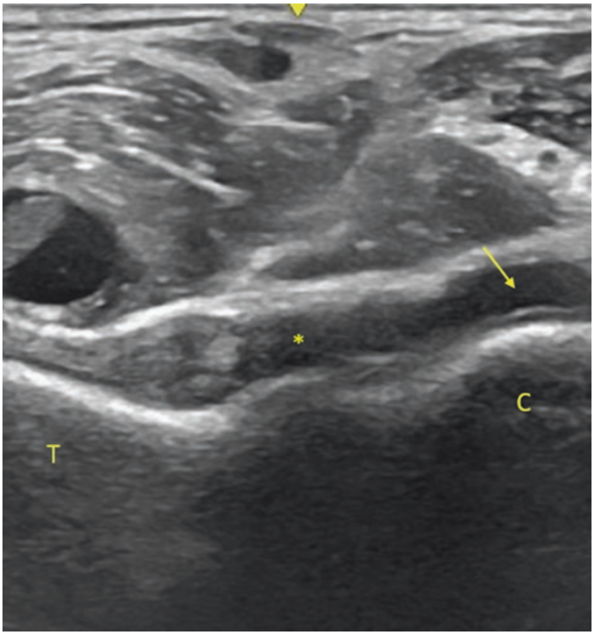

Fig. 4.13 Anterior transverse view of synovitis (*) of the elbow: trochlea (T) and capitellum (C). Notice the artifactual sharp hyperechoic thin interface sign (arrow) between the hyaline cartilage and overlying anechoic or hypoechoic material created by the difference in acoustic impedance between the two tissues

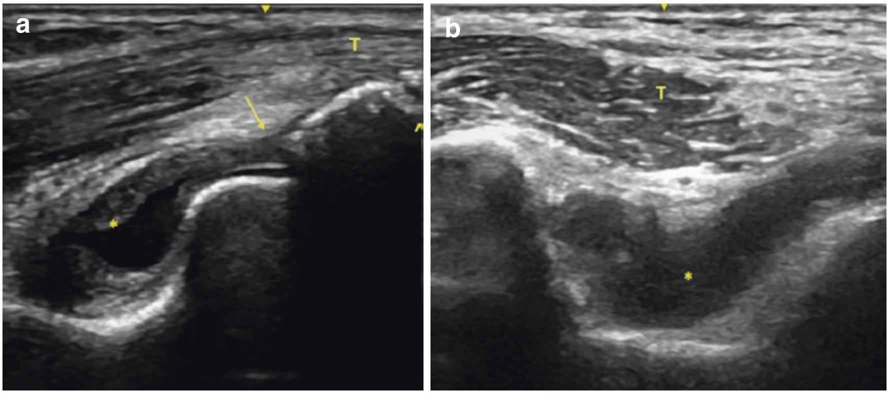

Fig. 4.14 Posterior longitudinal (**a**) and transverse (**b**) view of the elbow showing synovitis with effusion of the olecranon recess (*) in a patient with spondyloarthropathy. Triceps (T), olecranon (O), joint cleft (arrow)

be noted how the thickened synovium or fluid separates the joint capsule from the bone surface and displaces the fibrofatty tissue from the joint cleft.

Distinguishing synovial hypertrophy from an effusion may be challenging as both present as hypoechoic or anechoic tissue within the intra-articular space. However, synovial hypertrophy is not displaceable and poorly compressible and may or may not exhibit Doppler signal. In contrast, synovial effusion is more frequently anechoic and is displaceable and fully compressible and should not exhibit Doppler signal [6] (Fig. 4.16).

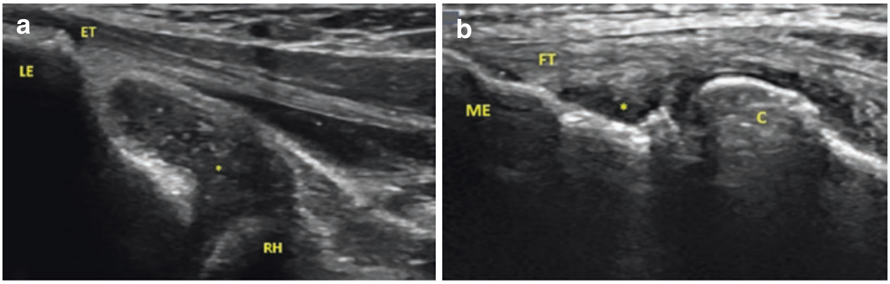

Fig. 4.15 Longitudinal views of synovitis (*) emerging from the lateral (**a**) and medial (**b**) joint cleft. Extensor tendon (ET), lateral epicondyle (LE), radial head (RH), flexor tendon (FT), medial epicondyle (ME), coronoid (C)

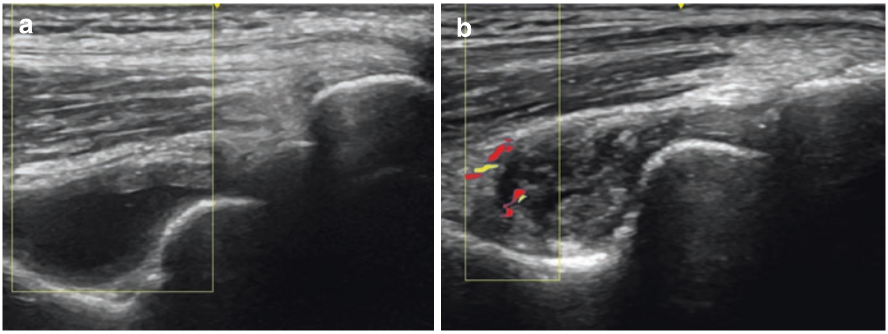

Fig. 4.16 Posterior longitudinal views of the olecranon fossa of two different cases. Picture (**a**) shows an anechoic effusion that is fully compressible and does not show Doppler signal. Contrast to picture (**b**) that shows hypoechoic synovium that is poorly compressible and may present Doppler signal. In both examples, the fat pad will be displaced anteriorly

Synovitis, on the other hand, is described as the presence of hypoechoic synovial hypertrophy regardless of the presence of effusion or any grade of Doppler signal. In many cases of inflammatory arthritis, the combination of both synovial hypertrophy and effusion is noted in conjunction (Fig. 4.17a, b). In contrast, an effusion (Fig. 4.16a) can be clearly distinguished from synovitis with power Doppler signal (Fig. 4.16b).

Small amounts of fluid initially collect in the olecranon fossa and are best visualized with the elbow in flexion. As the pathologic synovial process increases, there is elevation of the anterior and posterior fat pad creating a crescent-shaped appearance of the fat pad. On elbow extension, the fat pad will be compressed by the overlying brachialis muscle against the bone leading to less fluid collecting in the anterior coronoid and radial recess compared to elbow flexion. In markedly distended joints, anterior bulging of the joint cavity is noted and may extend down to the joint recess (Fig. 4.18b) [4, 7]. The recesses located inferiorly to the anterior fat pad, including the annular recess, tend to fill in cases of large amounts of joint effusion.

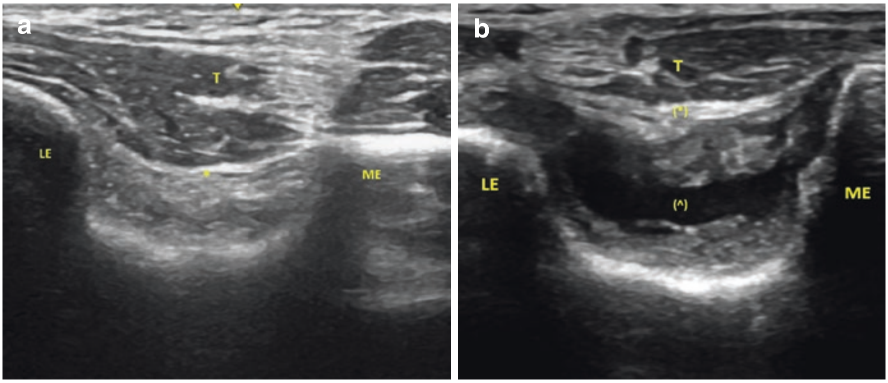

Fig. 4.17 (**a**) Transverse images over the posterior olecranon recess in a normal subject with normal hyperechoic fat occupying the fossa between the lateral (LE) and medial (ME) epicondyle. (**b**) Patient with an anechoic effusion (^) within hypoechoic synovium distending the olecranon recess (*). Fat pad should not be confused with synovitis or effusion. In doubtful cases, dynamic examination with elbow flexion and extension may help distinguish these conditions

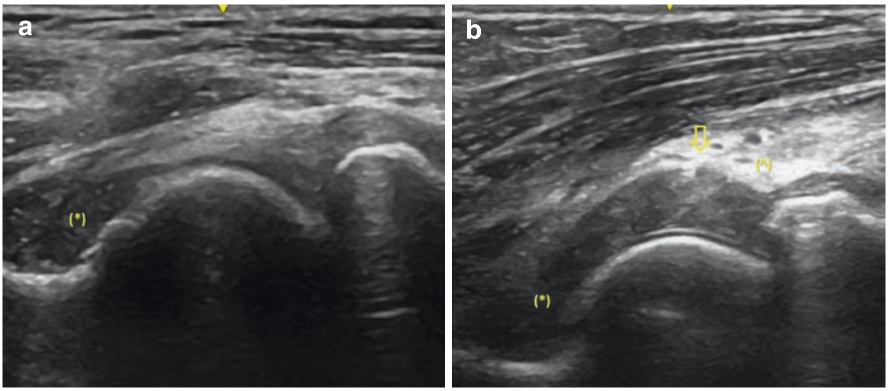

Fig. 4.18 Synovitis of the elbow: anterior longitudinal view. (**a**) Mild synovitis that is initially noted occupying the radial recess (*). (**b**) As joint fluid of synovium increases, the anterior fat pad is displaced anteriorly creating a characteristic crescent shape (^) with anterior bulging of the joint cavity more distally (open arrow)

Although ultrasound is optimal in identifying synovitis in evaluation of the elbow, there are no pathognomonic sonographic features that will distinguish among various forms of inflammatory arthritis. Nonetheless, there may be additional findings that may distinguish between different crystal-related arthropathies. The presence of tophus, double-contour sign, hyperechoic aggregates, and erosion are elementary lesions noted on ultrasound to have reliability in the diagnosis of gout [8–10] (Fig. 4.19).

In cases of calcium pyrophosphate deposition disease (CPPD), hyperechoic deposits of variable shape and size within the fibrocartilage or hyaline cartilage,

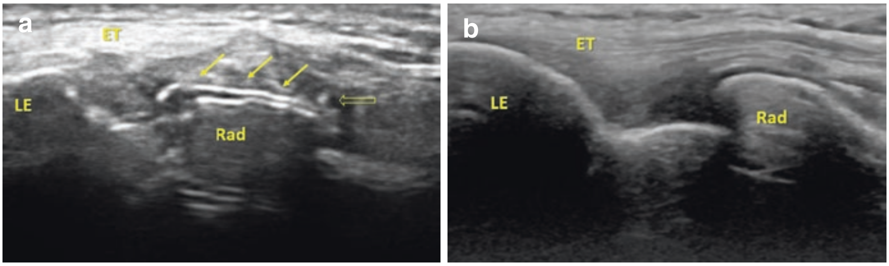

Fig. 4.19 Gouty-related findings of a lateral longitudinal elbow (**a**) distorted bony landmarks, hyperechoic aggregates (open arrow), and double-contour sign (arrows). Figure (**b**), normal lateral longitudinal elbow view. Lateral epicondyle (LE), extensor tendon (ET), radial head (Rad)

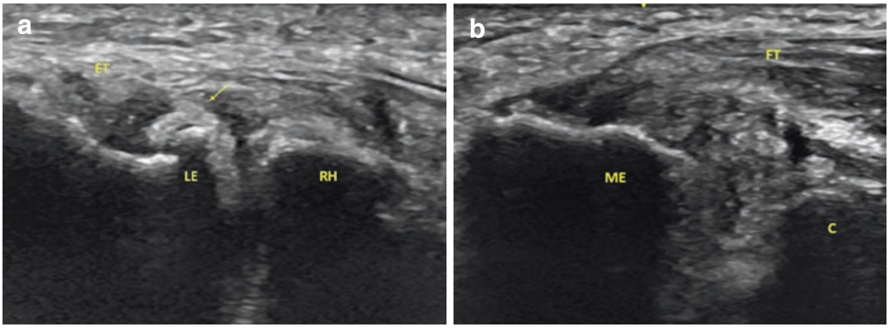

Fig. 4.20 Images of CPPD deposition. (**a**) Longitudinal view of the lateral elbow: there is a dense hyperechoic density in the intra-articular space over the lateral epicondyle (LE). (**b**) Longitudinal view of the medial elbow: bulkier hyperechoic densities at the joint cleft between the medial epicondyle (ME) and the coronoid (C). The flexor tendon exhibits hypoechoic swelling and thickening with anechoic gap from tear at the distal insertion. Note the smaller punctate hyperechoic CPPD densities scattered within the synovium in both images

linear deposits in tendons, or mobile punctate to large deposits in synovial fluid are among the various findings identified through sonography (Fig. 4.20). The medial meniscus and femoral condyle hyaline cartilage of the knee are considered the most frequently involved sites, but any joint, including the elbow, may be affected [11].

Bursal Pathology

The elbow has various bursae that are typically not visible through ultrasound in normal conditions. The most commonly visualizable olecranon bursa is evaluated with the elbow extended ideally floating the transducer with a thick layer of gel and minimal pressure to avoid displacing fluid from the field of view (Fig. 4.21). The olecranon bursa can be pathologically distended with fluid or synovium of variable echogenicity in cases of inflammatory or crystal-related arthritis, traumatic or septic bursitis, and possible concomitant soft tissue cellulitis (Fig. 4.22). Similar to what

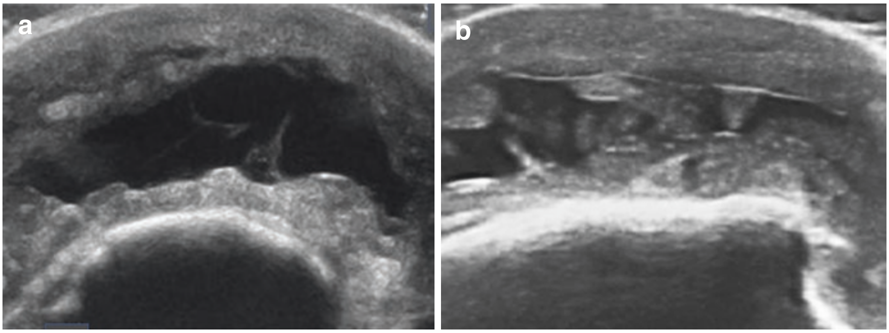

Fig. 4.21 (**a**) Olecranon bursitis with predominantly anechoic fluid and thickened synovial walls. (**b**) Chronic olecranon bursitis distended mostly by hypoechoic tissue hypertrophy and thickened bursal wall

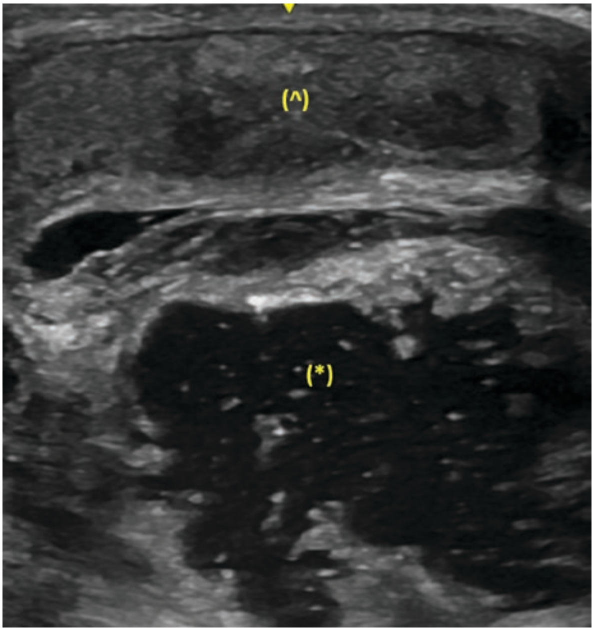

Fig. 4.22 Olecranon bursitis in a patient with severe rheumatoid arthritis. Transverse image reveals a painless heterogeneous soft-tissue mass (*) with mixed echotexture located in the subcutaneous tissue of the olecranon. Note the homogeneous rheumatoid nodule overlying the distended olecranon bursa

can be seen in the joint recess, hypoechoic complex fluid can be distinguished from tissue hypertrophy by the presence of compressibility, redistribution, or motion of bursal contents with transducer pressure and absence of Doppler flow. Identification of well-defined borders of a bursa and characteristic location may help differentiate a bursal collection from a joint effusion or abscess. Ultrasound features of olecranon bursitis are nonspecific, and there are no characteristic findings to definitively establish the etiology of bursal swelling. Sometimes a few crystals can be seen floating in effusion; however, aspiration is necessary to clarify whether fluid is infected and/or define crystalline contribution of bursitis. Ultrasound-guided aspirations can facilitate evacuation of fluid and loculated fluid collections or in cases where there is extensive tissue hypertrophy obstructing the needle.

A less frequently encountered bursa is the bicipitoradial bursa that does not communicate with the joint cavity and is found on the anterior aspect of the elbow adjacent to the distal biceps tendon attachment onto the radial tuberosity. Bicipitoradial bursitis presents as an anechoic formation surrounding the distal biceps tendon at the cubital fossa that can be accompanied by neurological symptoms caused by compression of the radial nerve. Ultrasound not only is useful in diagnosing the inflamed bursa but also can provide information about radial nerve injury and be used for guidance of therapeutic intrabursal aspiration and injection [12].

Tendon and Ligament Pathology

Lateral and medial epicondylitis is a misnomer that mostly describes degeneration, swelling, and at times microtearing of the common extensor/flexor tendon rather than true inflammation. It is a condition that can be diagnosed easily through physical exam, but ultrasound can aid by confirming the clinical diagnosis in doubtful or refractory cases, to qualitatively reveal the extent and severity of the disease and to monitor the response to therapy. The main ultrasound features noted are pre-insertional hypoechoic swelling of the tendon with loss of the fibrillar pattern (tendinosis), fluid adjacent to the common tendon, ill-defined tendon margins, adjacent bone irregularity, and on occasions hyperechoic calcification. The extensor carpi radialis brevis component of the common extensor tendon located at the most anterior portion of the tendon is found to be the most commonly affected (Fig. 4.23). Sonographic findings of intratendinous calcification, tendon thickening, adjacent bone irregularity, focal hypoechoic regions, and diffuse heterogeneity have been proven to correlate with symptom severity [15] (see Figs. 4.23 and 4.24 for examples of these elementary lesions).

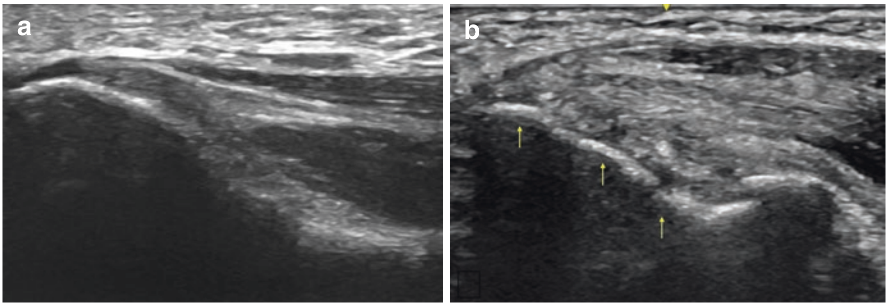

Fig. 4.23 Medial longitudinal view of the elbow. (**a**) Normal flexor tendon with linear fibrillar pattern of the tendon and attachment at bone is clearly delineated. (**b**) Hypoechoic thickening with loss of the fibrillar pattern of the tendon consistent with tendinosis. Note the increased convexity or bowing at the surface of the tendon caused by swollen fibers as well as small superimposed anechoic interstitial tears at portions of the tendon insertion (arrows)

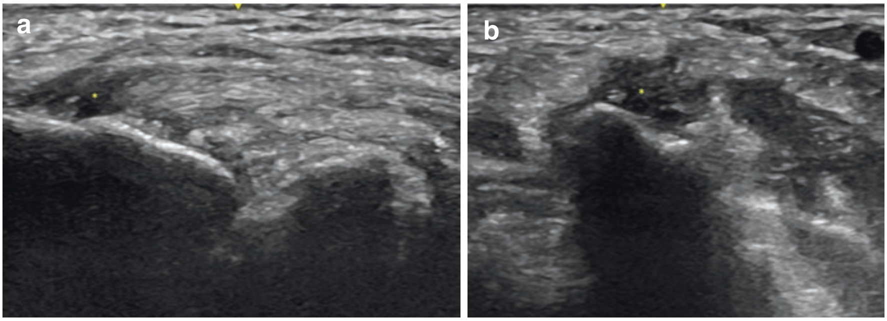

Fig. 4.24 Lateral extensor tendon insertional tear. (**a**) Longitudinal view of a common extensor tendon tear: anechoic interruption of the fibers at the superior attachment (extensor carpi radialis brevis component of the tendon) of the tendon that do not correct upon adjusting probe to exclude anisotropy. (**b**) Transverse view of a common extensor tendon tear for confirmation

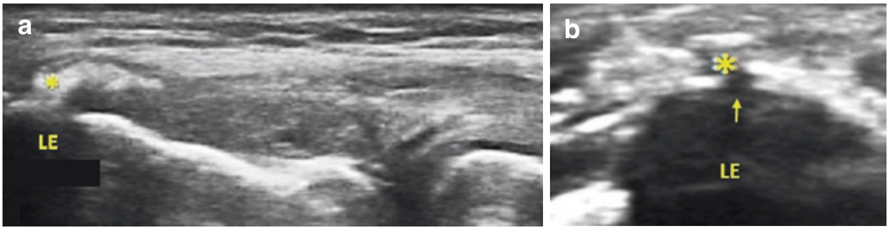

Fig. 4.25 Lateral extensor tendon calcification. Longitudinal (**a**) and transverse (**b**) view of a common extensor tendon showing linear calcification (*) that connects to the bone and can be seen in cases of chronic tendinosis. Note in image (**b**) acoustic shadowing (arrow) casted by the mature calcification

Intratendinous calcification or enthesopathy may be present in cases of chronic tendinosis (Fig. 4.25) [13, 14]. In cases of enthesophytes (Fig. 4.26), calcifications appear as hyperechoic spurs forming at a tendon insertion into the bone, growing in the direction of the natural pull of the tendon involved. Distinguishing mechanical vs. inflammatory calcifications may be challenging, and at times, it may be necessary to seek additional inflammatory features as well as correlate findings with clinical history and exam for a more conclusive assessment.

An additional feature of non-inflammatory "epicondylitis" is the presence of neovascularization noted as Doppler signal within the tendon substance that is a consequence of an angiofibroblastic hyperplasia with an immature reparative response (Fig. 4.27) In high-grade tendinosis, the angiofibroblastic infiltration secondary to migration of fibroblasts and vascular granulation tissue within the tendon substance causes a striking hypervascular pattern of the intratendinous hypoechoic areas [16] that should not be misinterpreted as enthesitis seen in inflammatory arthritis.

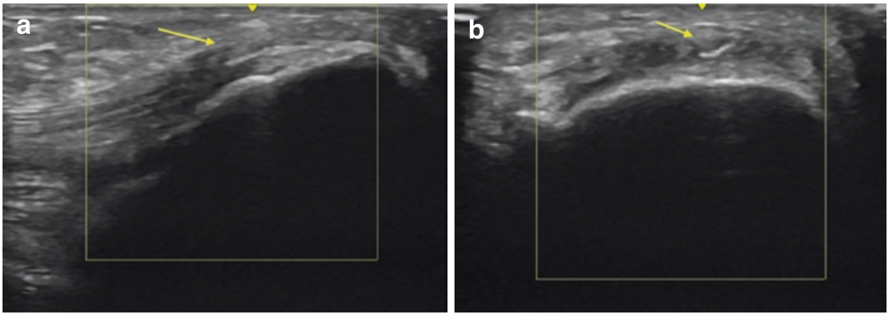

Fig. 4.26 Enthesophyte near triceps tendon of a patient with spondyloarthropathy. Posterior longitudinal (**a**) and transverse (**b**) view of a triceps tendon showing an enthesophyte appearing like a calcification (arrow); however, bony formation is seen connected to bony enthesis along the natural pull of the tendon

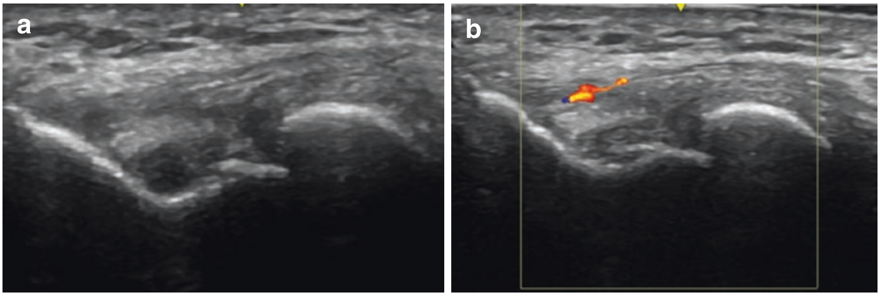

Fig. 4.27 (**a**) Lateral longitudinal view of a common extensor tendon at the lateral epicondyle showing hypoechoic tendinosis swelling of the tendon with anechoic interstitial tears. (**b**) View of the same tendon demonstrates power Doppler signal at the anechoic gaps from neovascularity signaling the tendons attempt to regenerate

Enthesitis is sonographically defined as hypoechoic and/or thickened insertion of the enthesis close to the bone (within 2 mm from the bony cortex) which exhibits Doppler signal if active and that may show erosions and enthesophytes/calcifications as sign of structural damage [8]. The detection of enthesitis with ultrasound is far more sensitive and specific than clinical examination in evaluating patients for spondyloarthropathies (SpA) [17]. Furthermore, ultrasound evaluation for enthesitis is reproducible and provides the means to quantify disease severity [18]. Various studies have included the triceps tendon or the common flexor or extensor tendon of the elbow as areas to evaluate for enthesitis in evaluating for SpA. The validity of ultrasound assessment evaluating elemental lesions of enthesis thickness, structure, calcifications, erosions, bursae, and power Doppler signal has been described for the diagnostic classification of SpA [19]. Distinction of non-inflammatory Doppler signal related to reparative neovascularization from that seen in inflammatory arthritis can be elusive at times. Detailed comparative studies of enthesis features in normal controls and patients with SpA have demonstrated absent power Doppler signal

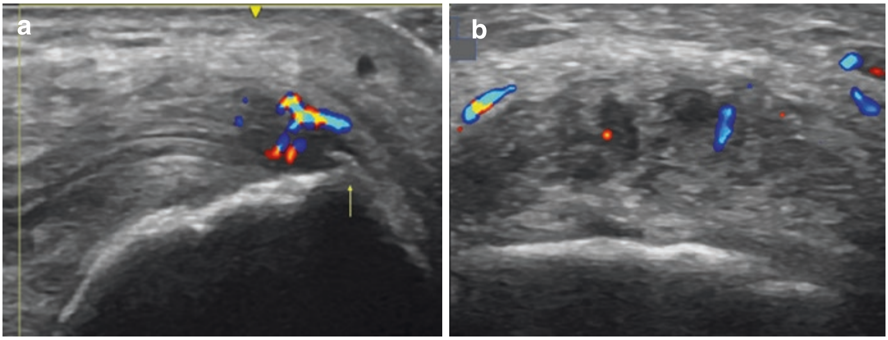

Fig. 4.28 Triceps tendon enthesitis in a patient with spondyloarthropathy. (**a**) Posterior longitudinal view of the triceps tendon showing heterogeneous thickening of the tendon with vascularization and cortical irregularities at its insertion to the olecranon. A small enthesophyte (arrow) noted as a hyperechoic spur forming at a tendon insertion into the bone growing in the direction of the natural pull of the tendon. (**b**) Same triceps tendon insertion changes on posterior transverse view

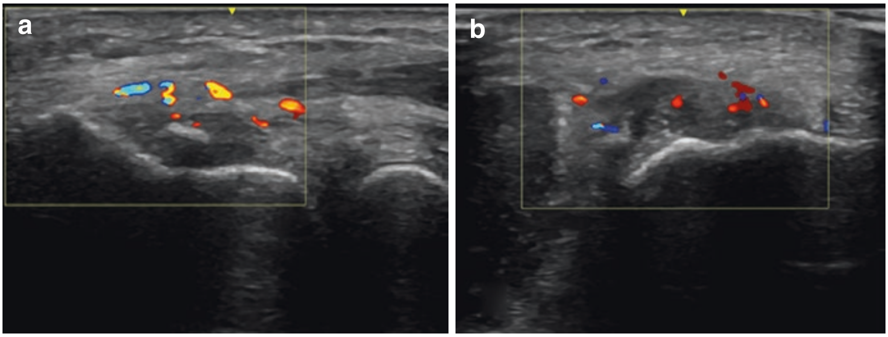

Fig. 4.29 Enthesitis of the common extensor tendon in a patient with psoriatic arthritis. (**a**) Longitudinal lateral view of the common extensor tendon at the lateral epicondyle showing tendon thickening with decreased echogenicity, positive power Doppler signal, and early cortical irregularities. (**b**) Transverse lateral view of the extensor tendon showing anechoic gaps, hypoechoic swelling, and positive power Doppler signal

of the abnormal entheses in control patients, whereas Doppler signal was seen in 81% of abnormal entheses of SpA patients. In patients with SpA, vascularization was usually detected at the cortical bone insertion and at times also in the bursa with no difference observed in the distribution of enthesis pattern between the distinct SpA subtypes [20] (see Figs. 4.28 and 4.29 for examples of enthesitis).

Ligaments of the elbow that can be evaluated by ultrasound include the anterior band of the ulnar collateral ligament (UCL) medially and laterally the lateral collateral ligament (LCL) and radial collateral ligament (RCL). A focal tear of the ligament may appear as focal hypoechoic heterogeneity and laxity with thickening of the ligament without complete ligament fiber disruption. In cases of complete tears, widening of the adjacent joint space can be noted with soft tissue falling into the distracted articular space with surrounding effusion slightly posterior and deep to the medial or lateral epicondyle. Comparative dynamic imaging with contralateral elbow demonstrating joint instability and ligament laxity can be exerted through valgus and varus stress for evaluation of UCL and varus LCL injury, respectively [15]. It is of interest to include evaluation of the overlying tendon as concomitant tears of the flexor or extensor tendon can occur as a result of the same forces or overuse mechanisms on adjacent structures.

Bony Pathology

Erosions seen in cases of inflammatory arthritis are usually seen as an intra-articular discontinuity of the bone surface that is visible in two perpendicular planes [8] (see Figs. 4.30 and 4.31).

Ultrasound of the elbow has been demonstrated to be useful for the detection of early changes in rheumatoid arthritis (Fig. 4.32). In early disease, soft tissue alterations and early erosions are better detected by sonography than by conventional

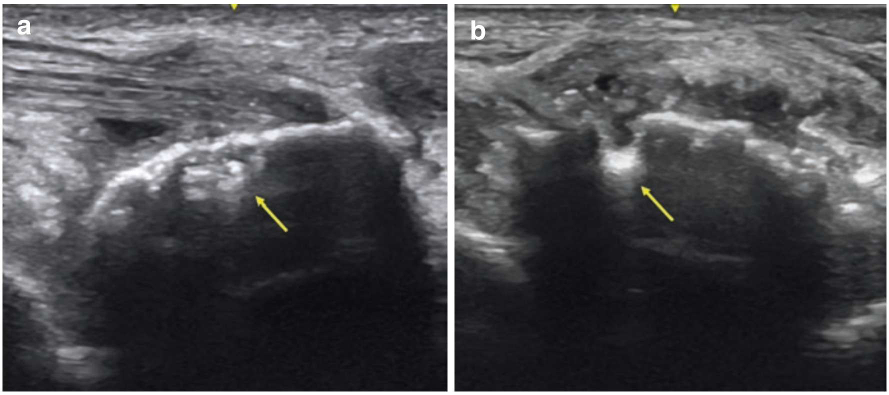

Fig. 4.30 Triceps tendon enthesitis and erosion in orthogonal planes. Longitudinal (**a**) and transverse (**b**) views of the triceps tendon enthesitis with a large punched out erosion (arrow) at the insertion of the tendon. Figure (**b**) shows a transverse view of the erosion and extensive cortical bone disruption observed at the level of the triceps insertion

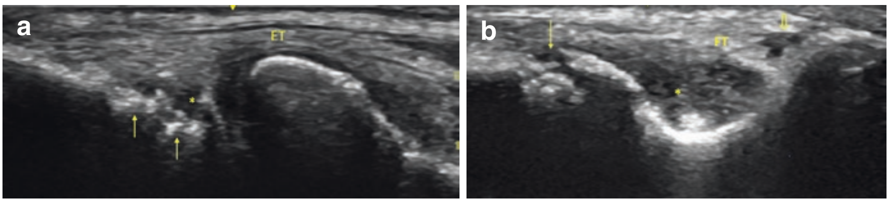

Fig. 4.31 Bony erosions (arrow) adjacent to site of emerging synovitis (*) from the lateral (**a**) and medial (**b**) joint cleft in a patient with rheumatoid arthritis. Flexor tendon *FT*, extensor tendon *ET*. Note in Figure b the presence of a tendon tear of the flexor tendon (open arrow)

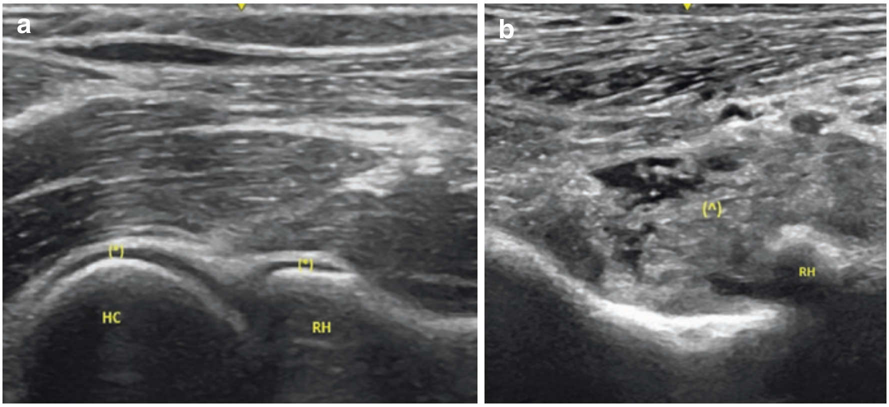

Fig. 4.32 Anterior longitudinal view of the radiocapitellar joint. (**a**) Normal. The articular cartilage (*) and the normal profile of the bone of the humeral capitellum (HC) and radial head (RH) can be clearly identified. (**b**) Destructive pannus in rheumatoid arthritis = grade 5 in a patient with severe rheumatoid arthritis. Note the complete loss of the cartilage and the eroded humeral capitellum (HC) and loss of the bony contours of the radial head (RH) distorting the classic bony landmarks. Proliferative synovial pannus (^) is noted on the surface of the joint distending the annular recess

radiography. A sonographic classification of rheumatoid joint destruction at the elbow to stage disease and identify early destructive process for both the prognosis and treatment strategy has been described: grade 0, normal condition; grade 1, joint effusion with capsular distension; grade 2, small erosion of the radial head with an irregular floor and joint cyst filled with pannus; grade 3, cortical defect of the humeral capitellum, joint effusion, and joint space narrowing; grade 4, cortical defect of the radial head and humeral capitellum; and grade 5, cortical destruction and loss of articular guide structures [21] (Fig. 4.32, 4.33).

Osteoarthritis in the elbow is seen as in other joints presenting with osteophytes as a cardinal feature. Osteophytes have a characteristic sonographic appearance as an irregularity or protuberance of the bony cortex localized in the borders of articular surfaces (Fig. 4.33). In addition, loss of echotexture, width, and definition of the borders of the adjacent cartilage can be identified [22] (Fig. 4.34).

Intra-articular loose bodies can at times be confused with osteophytes if found in close proximity to the bone. These can appear as a hyperechoic fragment that may be ossified and produce acoustic shadowing depending on its level of ossification. Dynamic flexion and extension of the elbow will result in mobilization of fluid and loose bodies that can help differentiate them from local heterotopic ossification or an osteophyte. The elbow is the second most common site of intra-articular bodies after the knee, where they typically present in dependent portions of the olecranon or coronoid fossa that can result in intermittent locking and loss of extension of the joint (Fig. 4.35) [16].

High-resolution ultrasound can be useful in detecting occult fractures missed on conventional radiography. Occult fractures will present as a “step-off” bone disruption or discontinuity of the bone surface (Fig. 4.35). Further diagnostic imaging with computed tomography or magnetic resonance may be considered for

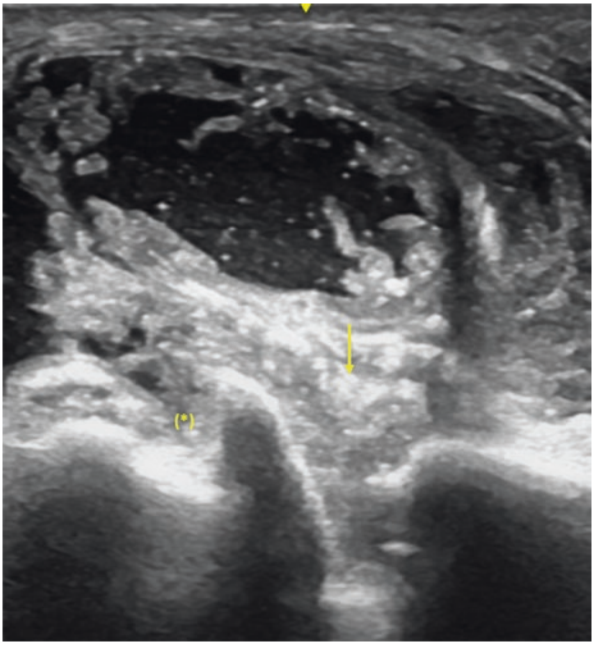

Fig. 4.33 Lateral longitudinal elbow view of a patient with rheumatoid arthritis showing synovitis with effusion. The lateral collateral ligament is not visualized and has been replaced by synovium protruding through the joint cleft between the lateral epicondyle and the radial head (arrow). Note the large erosion (*) of the lateral epicondyle giving the appearance of an osteophyte

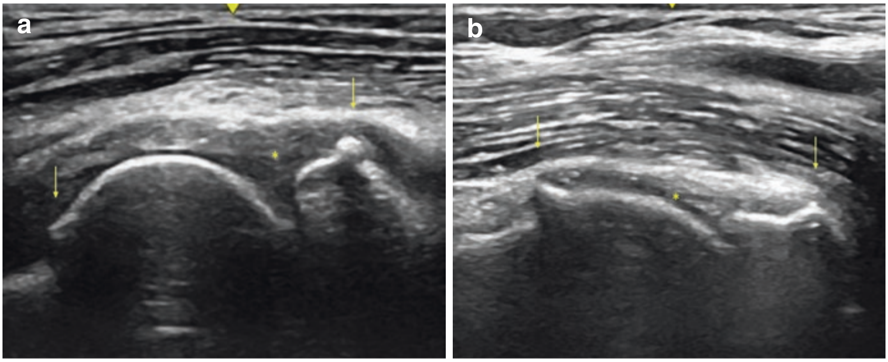

Fig. 4.34 Anterior longitudinal views of (**a**) humeroradial joint and (**b**) humeroulnar joint. Early osteophytic protuberance at the humeral head in both images with cartilage loss and osteophyte (arrows) at the radial head (**a**) and early deformity of the coronoid process in (**b**)

confirmation of fracture in suspected cases, particularly to clarify avulsion fracture. The hip, elbow, and ankle are the most common sites of avulsion fractures.

Soft Tissue Pathology

The posterior elbow is a common location to encounter various nodular lesions. The sonographic characteristics that distinguish gouty tophi from rheumatoid nodules

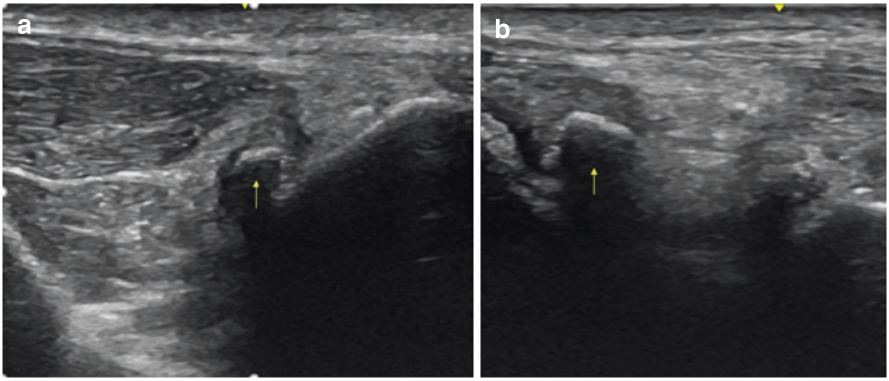

Fig. 4.35 Posterior longitudinal (**a**) and transverse (**b**) views of an intra-articular loose body (arrows) within the posterior fossa. Notice the posterior acoustic shadowing casted by the hyperechoic ossified loose body. There is no connection of the loose body to the olecranon. Dynamic maneuver with flexion and extension of the elbow can show a loose body may be displaceable, while an osteophyte will remain attached to the bone

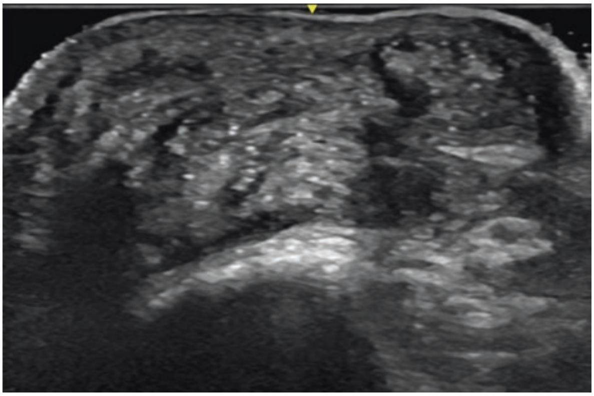

Fig. 4.36 Gouty tophus. Heterogeneous mass with ill-defined borders: hyperechoic punctate tophi admixed with hypoechoic areas thought to be due to chalky liquid material

have been well described. Gouty tophi will generally appear as irregularly shaped heterogeneous masses with the presence of hyperechoic densities from tophi that can occasionally show posterior acoustic shadowing in cases of calcified tophi from long established gout (Fig. 4.36). Cortical bone erosions adjacent to tophi can more frequently be noted in gout compared to rheumatoid nodules. In contrast, rheumatoid nodules appear as oval, generally homogeneous masses with hyperechogenic walls that are attached in close proximity to the bone and have less frequently associated erosive changes. Rheumatoid nodules can frequently present with a centrally sharp demarcated hypoechoic area that is thought to correspond to central necrosis (Fig. 4.37) [23].

Other soft tissue masses, including ganglion cysts and lymph nodes, and tumors, including and lipomas and sarcomas, can be found in various regions of the elbow. MRI and/or biopsy may be necessary for further investigation.

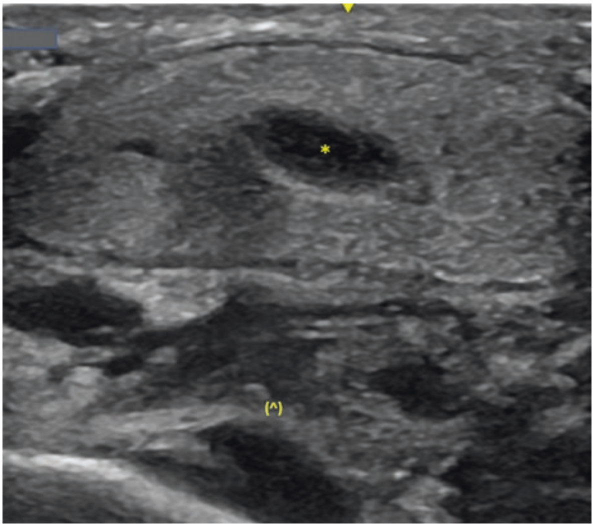

Fig. 4.37 Rheumatoid nodule. Homogeneous mass with well-defined borders and characteristic hypoechoic center (*) presumed to be due to central necrosis. In this case, the rheumatoid nodule is not in close proximity to the bone as typically described as it is overlying a distended olecranon bursa (^)

Nerve Pathology

Ultrasound is a feasible tool to evaluate the pathology of the ulnar nerve at the elbow. Entrapment of the ulnar nerve at the cubital tunnel is the second most common entrapment syndrome of the upper limb after carpal tunnel syndrome. The cubital tunnel encased superiorly by the retinaculum (Osborne's fascia) is identified transversely by placing one end of the probe on the medial epicondyle and the other end at the distal olecranon. Ulnar nerve entrapment can be seen as enlargement of the ulnar nerve just proximal to the cubital tunnel with hypoechoic swelling with loss of the normal speckled pattern of the nerve and, in some cases, hypervascularity with power Doppler imaging. A recent metanalysis "assessing" the ulnar nerve cross-sectional area (CSA) for the diagnosis of cubital tunnel syndrome concluded that a CSA of 10 mm^2 is a cutoff point for diagnosing ulnar nerve entrapment at the elbow region [24]. Ultrasound can also identify among several causes of ulnar nerve impingement, including bone abnormalities (fracture-related bony deformities, medial osteophytes, loose bodies, or heterotopic ossification), as well as the presence of space-occupying lesions, including invasive synovium, ganglia, lipoma, and cases of accessory anconeus epitrochlearis muscle that occurs in 23% of the population. (Figs. 4.38 and 4.39).

It is important to dynamically assess for subluxation of the ulnar nerve over the medial epicondyle with flexion and extension. This condition may predispose to nerve injury and irritation or in 20% be an asymptomatic condition, highlighting the importance of clinical correlation [18]. This maneuver at the same location can also help diagnose snapping triceps syndrome that may be accompanied by nerve subluxation (Fig. 4.40) [25].

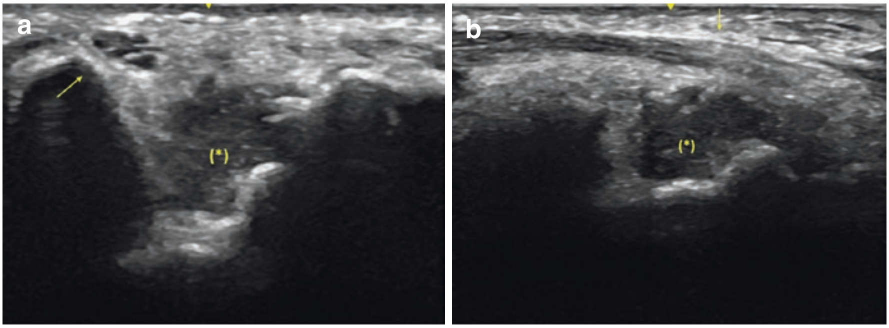

Fig. 4.38 Posteromedial view of the ulnar tunnel of the elbow: (**a**) transverse and (**b**) longitudinal views showing ulnar nerve (arrow) compression and displacement by synovial proliferation (*). Note in Figure (**b**) the area of pre-stenotic swelling and loss of fascicular pattern of the nerve as it enters the cubital/ulnar tunnel

Fig. 4.39 Transverse view of the cubital tunnel of the elbow with compressed ulnar nerve (^) from synovial proliferation (*) from calcium-related arthropathy (arrows)

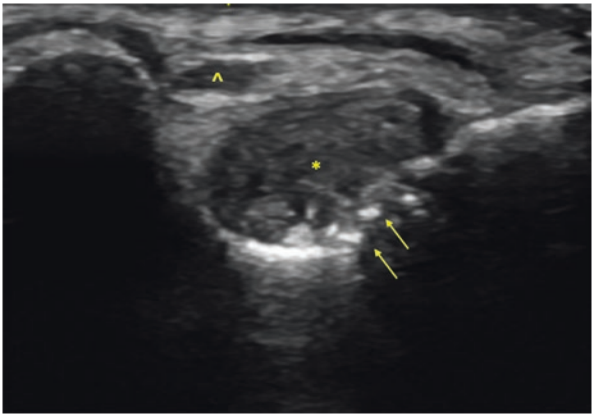

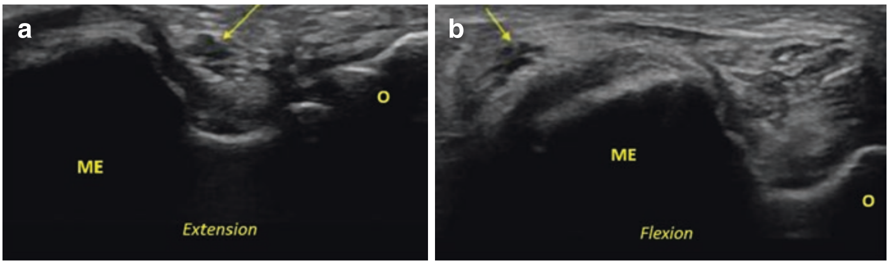

Fig. 4.40 Ulnar nerve subluxation. (**a**) Nerve within the ulnar tunnel with elbow in extension. (**b**) Translocation of the nerve over the medial epicondyle with elbow in full flexion

Ultrasound-Guided Procedures at the Elbow

Injection or aspiration of the elbow joint has been traditionally performed using clinical anatomic landmarks. Few studies have assessed the accuracy of palpation-guided injections (PGI) with that of ultrasound-guided injections (USGI) [26, 27]. A small study by Kim and colleagues reported an accuracy rate of 100% of USGI by posterior approach compared to 77.5% accuracy rate of PGI after confirmation by fluoroscopy in elbows of patients with osteoarthritis [29]. Available literature favors the posterior approach as the posterior olecranon recess is the most sensitive location to identify fluid [4], and there is less risk of vascular or nerve injury when approaching posteriorly. Posterior elbow joint injection is performed with the elbow flexed 90 degrees introducing the needle in plane longitudinally targeting the olecranon fossa or the needle can be introduced via transverse approach laterally to target the olecranon fossa (Fig. 4.41).

In refractory cases of lateral epicondylosis where conventional therapy is ineffective, ultrasound (US)-guided injection therapies have become of increasing interest. Positioning of the patient for USGI of the common extensor tendon is with the elbow flexed 90 degrees with the forearm prone with the transducer placed at the long axis of the tendon. The needle is advanced from distal to proximal direction. Depending on the injectate, the needle target may vary from peritendinous to intratendinous (Fig. 4.42).

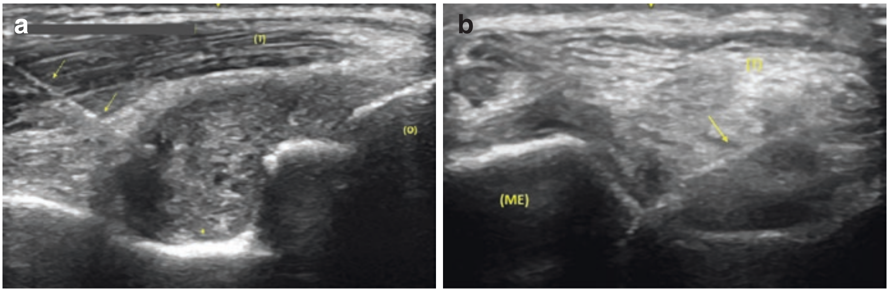

Fig. 4.41 Ultrasound-guided elbow injection through posterior longitudinal (**a**) and transverse (**b**) approaches

Fig. 4.42 Example of common extensor injection through in-plane lateral longitudinal approach

The literature regarding efficacy of individual approaches of US-guided treatment including needle tenotomy, prolotherapy, autologous whole blood injection (AWB), platelet-rich plasma (PRP) injection, and steroid injection is currently unclear. A systematic review of needle tenotomy demonstrated improvement in pain, but studies have not included placebo or control groups. McShane and colleagues have demonstrated superior results of US-guided tenotomy without administration of corticosteroid after tendon fenestration after a prior trial by the same group that was followed routinely by corticosteroid injection [28, 29]. PRP therapy has demonstrated a statistically significant improvement in pain and functionality for refractory lateral epicondylitis in a systematic review performed in 2013. AWB injection has been evaluated through well-designed studies to show statistically significant reductions in pain. Prolotherapy studies have also reportedly been of some benefit, although a recent study looking at prolotherapy in combination with physiotherapy vs. physiotherapy alone showed no significant differences in pain and function [30]. Nonetheless, no clear conclusions can be drawn at this time of a preferred approach among these methods for the management of degenerative tendon pathology [31]. Notably, corticosteroid injections for lateral epicondylitis, while once standard of care and helpful in short-term symptoms, have fallen out of favor and may lead to worse outcomes in long-term management with results showing inferior outcome and higher recurrence rate at 1 year [32].

Aspiration or injection of the olecranon bursa can often be easily performed without needle guidance. However, ultrasound can assist in successfully guiding needle placement in cases where there is significant synovial thickening and septations to ensure maximal drainage and accurate corticosteroid placement when indicated (Fig. 4.43).

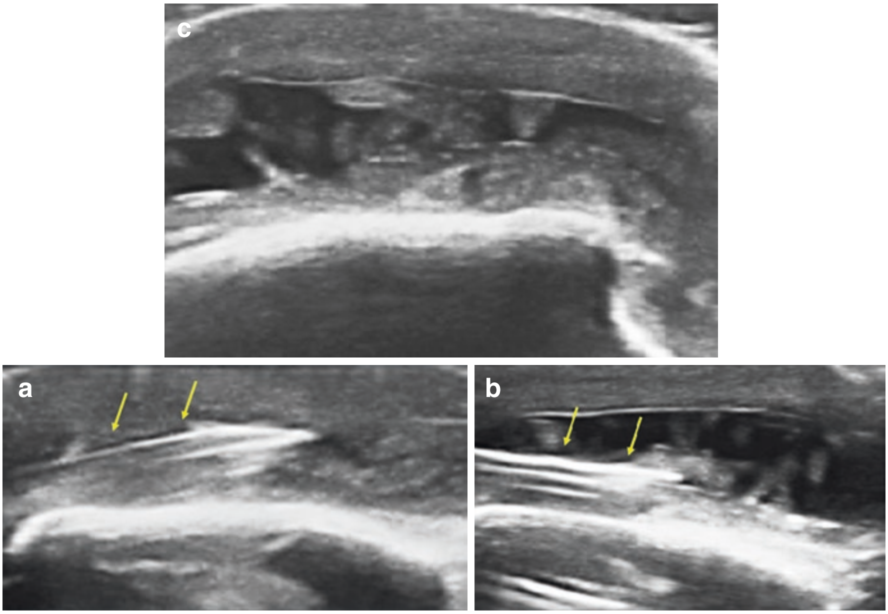

Fig. 4.43 (**a**) Olecranon bursitis, (**b**) needle placement during aspiration, (**c**) successful evacuation of fluid

Conclusion

Ultrasound is an invaluable tool that can be used to evaluate for various elbow pathologic conditions. The spectrum of additional information that can be obtained in various rheumatic conditions exceeds that obtained from radiography, and the costs and convenience are preferable over magnetic resonance. Complementing evaluation with elbow sonography can enhance diagnostic and procedural accuracy leading to improved management and outcomes of elbow disorders.

Review Questions

1. The following longitudinal view of the elbow demonstrates distention of which of the following joint recesses/fossa?

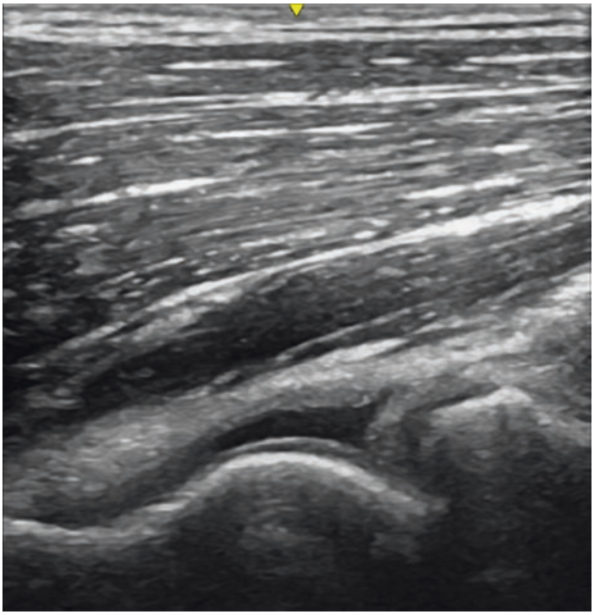

   (a) Olecranon fossa
   (b) Annular fossa
   (c) Radial fossa
   (d) Coronoid fossa

2. Identify the site of the effusion in this posterior longitudinal view of the elbow.

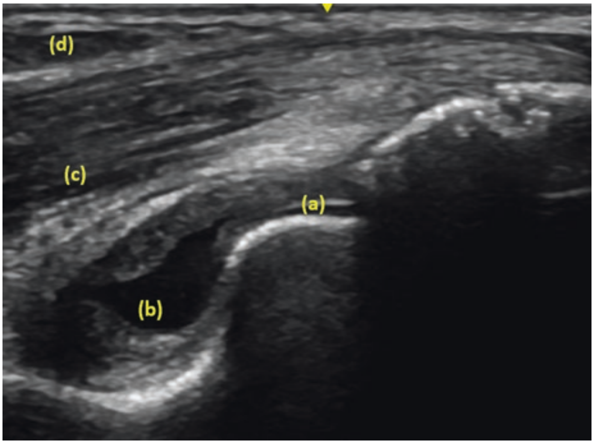

3. Identify the descriptive features of this soft tissue abnormality at the olecranon with its associated diagnosis.

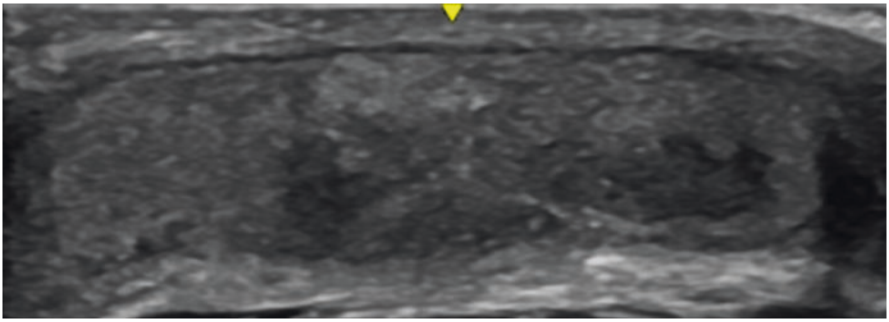

(a) Subcutaneous hypoechoic/anechoic compressible material: olecranon bursa effusion
(b) Heterogeneous irregular mass with hyperechoic densities: tophus
(c) Diffuse thickening of the dermis with edema and anechoic fat stranding: cellulitis
(d) Homogeneous well-defined mass with hypoechoic center: rheumatoid nodule

4. The following image is viewed by which of the following probe positions?

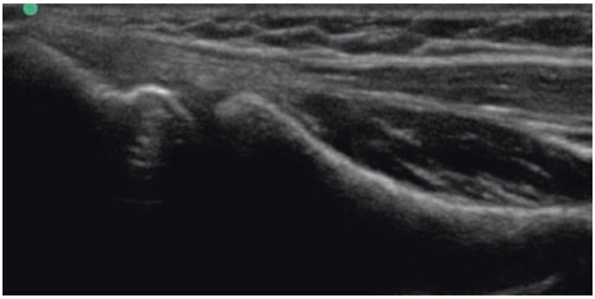

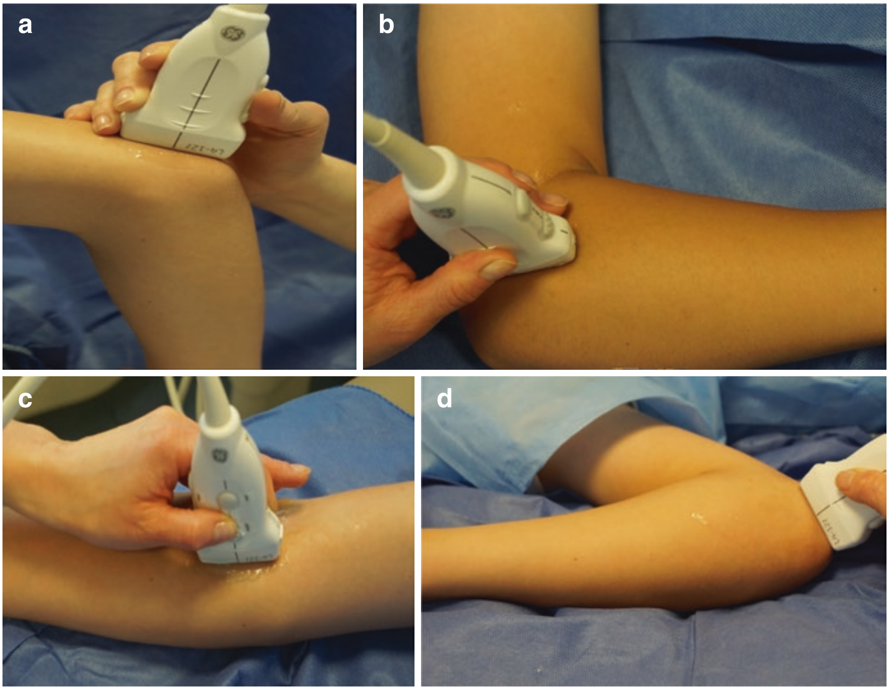

5. Which of the following markings is *not* associated properly with the corresponding anatomical structure on this anterior transverse view of the elbow?

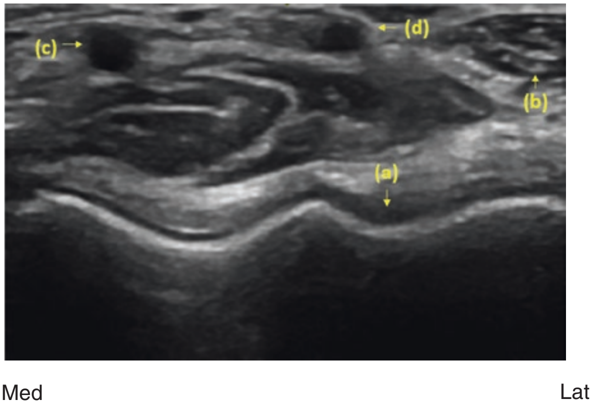

   (a) Articular cartilage
   (b) Brachialis muscle
   (c) Brachial artery
   (d) Biceps brachii tendon
6. Identify the dynamic maneuver that will enhance the detection of a tear of the radial collateral ligament.
   (a) Flexion extension
   (b) Valgus stress
   (c) Supination pronation
   (d) Varus stress
7. Which feature of this longitudinal view of the lateral extensor tendon is most suggestive of inflammatory enthesitis?

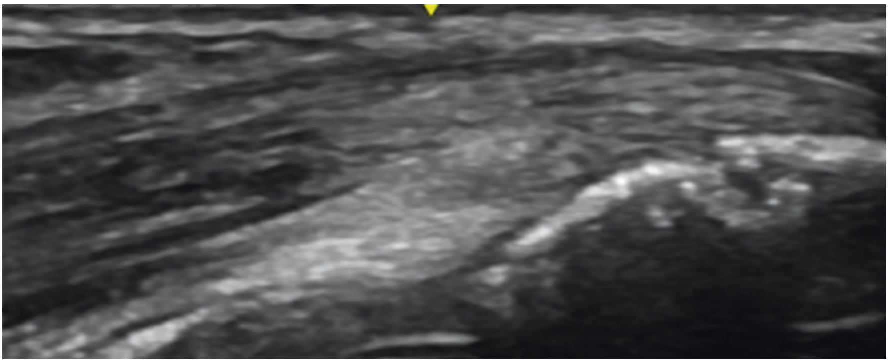

   (a) Diffuse thickening of the tendon
   (b) Loss of tendon fibrillar pattern
   (c) Erosion at the tendon insertion
   (d) Disruption of the tendon fibers

8. The presence of which of the mentioned characteristics of abnormal intra-articular material in this anterior transverse view of the elbow joint will *not* be seen in an effusion and may be seen in synovitis?

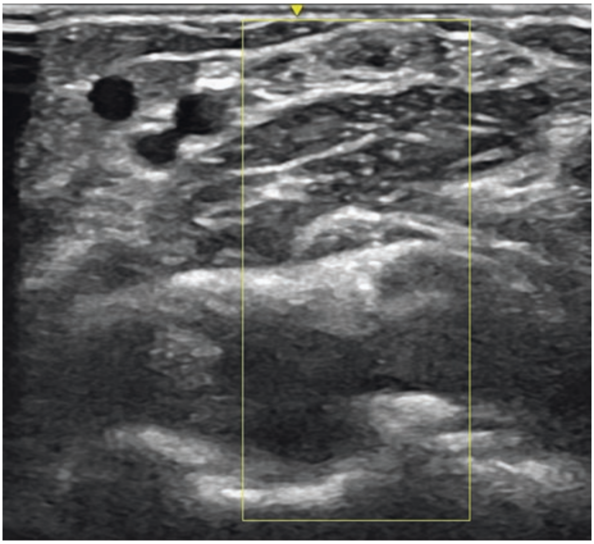

   (a) Compressibility
   (b) Varying echogenicity
   (c) Presence of Doppler signal
   (d) Displacement of fat pad
9. Select the option that can best optimize the visibility of the distal insertion of the biceps brachii tendon in this anterior longitudinal view of the elbow.

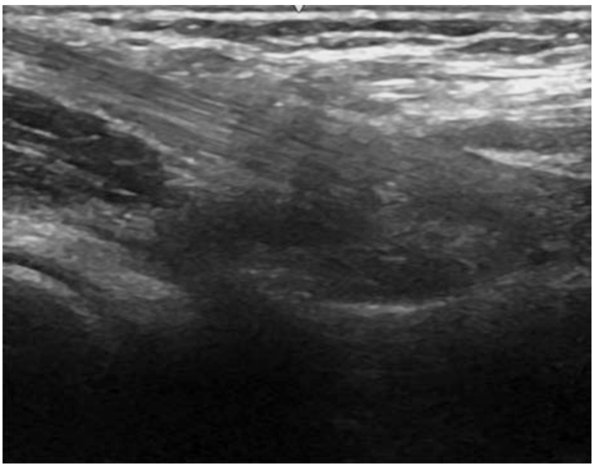

   (a) Increasing the pressure at the distal end of the probe (heel-toe)
   (b) Increasing the depth of the image
   (c) Tilting the probe side to side (rock the probe)
   (d) Decreasing the gain of the image
10. The following image of the posterior elbow longitudinal (left image) and transverse (right image) view is demonstrating?

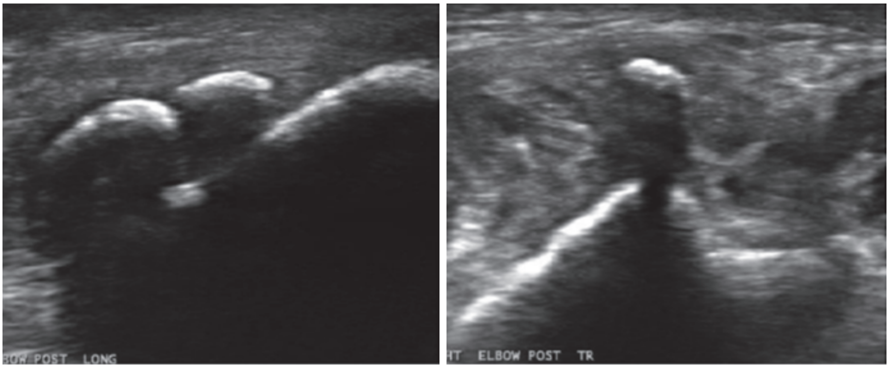

   (a) Degenerative osteophyte
   (b) Tendon enthesophyte
   (c) Intra-articular loose body
   (d) Double-contour sign: gout

Answers
1. (d) Coronoid fossa
2. (b)
3. (d) Homogeneous well-defined mass with hypoechoic center: rheumatoid nodule
4. (b)
5. (b) Brachialis muscle
6. (d) Varus stress
7. (b) Erosion at the tendon insertion
8. (c) Presence of Doppler signal
9. (a) Increasing the pressure at the distal end of the probe (heel-toe)
10. (c) Intra-articular loose body

References

1. Miles KA, Lamont AC. Ultrasonic demonstration of the elbow fat pads. Clin Radiol. 1989;40(6):602–4.
2. Jacobson J. Elbow ultrasound. In: Fundamentals in musculoskeletal ultrasound. 3rd ed. Philadelphia: Elsevier; 2017. p. 127–67.

3. De Smet AA, Winter TC, Best TM, Bernhardt DT. Dynamic sonography with valgus stress to assess elbow ulnar collateral ligament injury in baseball pitchers. Skeletal Radiol. 2002;31(11):671–6.
4. De Maeseneer M, Jacobson JA, Jaovisidha S, Lenchik L, Ryu KN, Trudell DR, Resnick D. Elbow effusions: distribution of joint fluid with flexion and extension and imaging implications. Invest Radiol. 1998;33(2):117–25.
5. Luukkainen R, Sanila MT, Saltyshev M, Huhtala H, Koski JM. Relationship between clinically detected joint swelling and effusion diagnosed by ultrasonography in elbow joints in patients with rheumatoid arthritis. Clin Rheumatol. 2005;24(3):228–31.
6. Wakefield RJ, Balint PV, Szkudlarek M, et al. Musculoskeletal ultrasound including definitions for ultrasonographic pathology. J Rheumatol. 2005;32(12):2485–7.
7. O'Neill J. The elbow. In: Musculoskeletal ultrasound: anatomy and technique. New York: Springer; 2008. p. 77–101.
8. Bruyn GA, Iagnocco A, Naredo E, et al. OMERACT definitions for ultrasonographic pathologies and elementary lesions of rheumatic disorders 15 years on. J Rheumatol. 2019;1. Epub ahead of print.
9. Thiele RG, Schlesinger N. Diagnosis of gout by ultrasound. Rheumatology. 2007;46(7):1116–21.
10. Cazenave T, Martire V, Reginato AM. Reliability of OMERACT ultrasound elementary lesions in gout: results from a multicenter exercise. Rheumatol Int. 2019;39(4):707–13.
11. Filipppou G, Scire C, Damjanov N, et al. Definition and reliability assessment of elementary ultrasonographic findings in calcium pyrophosphate deposition disease: a study by the OMERACT calcium pyrophosphate deposition disease ultrasound task force. J Rheumatol. 2017;44(2):1744–9.
12. Draghi F, Gregoli B, Sileo C. Sonography of the bicipitoradial bursa: a short pictorial essay. J Ultrasound. 2012;15(1):39–41.
13. Levin D, Nazarian LN, Miller TT, O'Kane PL, Feld RI, Parker L, McShane JM. Lateral epicondylitis of the elbow: US findings. Radiology. 2005;237(1):230–4.
14. Connell D, Burke F, Coombes P, et al. Sonographic examination of lateral epicondylitis. AJR Am JRoentgenol. 2001;176(3):777–82.
15. Konin GP, Nazarian LN, Walz DM. US of the elbow: indications, technique, normal anatomy, and pathologic conditions. Radiographics. 2013;33(4):E125.
16. Bianchi S, Martinoli C. Elbow. In: Bianchi S, Martinoli C, eds. Ultrasound of the musculoskeletal system, New York, : Springer, 2007; pp 349–408.
17. Balint PV, Kane D, Wilson H, McInnes IB, Sturrock RD. Ultrasonography of entheseal insertions in the lower limb in spondyloarthropathy. Ann Rheum Dis. 2002;61:905–10. 9.
18. Alcalde M, Acebes JC, Cruz M, Gonzalez-Hombrado L, Herrero-Beaumont G, Sanchez-Pernaute O. A Sonographic Enthesitic Index of lower limbs is a valuable tool in the assessment of ankylosing spondylitis. Ann Rheum Dis. 2007;66:1015–9.
19. de Miguel E, Cobo T, Muñoz-Fernández S, et al. Validity of enthesis ultrasound assessment in spondyloarthropathy. Ann Rheum Dis. 2009;68(2):169–74.
20. D'Agostino MA, Said-Nahal R, Hacquard-Bouder C, Brasseur JL, Dougados M, Breban M. Assessment of peripheral enthesitis in the spondyloarthropathies by ultrasonography combined with power Doppler. A cross-sectional study. Arthritis Rheum. 2003;48:523–33. 10.
21. Lerch K, Borisch N, Paetzel C, Grifka J, Hartung W. Sonographic evaluation of the elbow in rheumatoid arthritis: a classification of joint destruction. Ultrasound Med Biol. 2003;29(8):1131–5.
22. Guinsburg M, Ventura-Ríos L, Bernal A, Hernández-Díaz C, Pineda C. Usefulness, validity, and reliability of ultrasound in the diagnosis of osteoarthritis: a critical review of the literature. Gac Med Mex. 2013;149(5):509–20.
23. Nalbant S, Corominas H, Hsu B, Chen LX, Schumacher HR, Kitumnuaypong T. Ultrasonography for assessment of subcutaneous nodules. J Rheumatol. 2003;30(6):1191–5.

24. Chang KV, Wu WT, Han DS, Özçakar L. Ulnar nerve cross-sectional area for the diagnosis of cubital tunnel syndrome: a meta-analysis of ultrasonographic measurements. Arch Phys Med Rehabil. 2018;99(4):743–57.
25. Jacobson JA, Jebson PJ, Jeffers AW, Fessell DP, Hayes CW. Ulnar nerve dislocation and snapping triceps syndrome: diagnosis with dynamic sonography: report of three cases. Radiology. 2001;220(3):601–5.
26. Balint PV, Kane D, Hunter J, et al. Ultrasound guided versus conventional joint and soft tissue fluid aspiration in rheumatology practice; a pilot study. J Rheumatol. 2002;29(10):2209–13.
27. Kim TK, Lee JH, Park KD, et al. Ultrasound versus palpation guidance for intra-articular injections in patients with degenerative osteoarthritis of the elbow. J Clin Ultrasound. 2013;41(8):479–85.
28. McShane JM, Shah VN, Nazarian LN. Sonographically guided percutaneous needle tenotomy for treatment of common extensor tendinosis in the elbow: is a corticosteroid necessary? J Ultrasound Med. 2008;27(8):1137–44.
29. McShane JM, Nazarian LN, Harwood MI. Sonographically guided percutaneous needle tenotomy for treatment of common extensor tendinosis in the elbow. J Ultrasound Med. 2006;25(10):1281–9.
30. Yelland M, Rabago D, Ryan M, et al. Prolotherapy injections and physiotherapy used singly and in combination for lateral epicondylalgia: a single-blinded randomised clinical trial. BMC Musculoskelet Disord. 2019;20:509.
31. Shergill R, Choudur HN. Ultrasound-guided interventions in lateral epicondylitis. J Clin Rheumatol. 2019;25(3):e27–34.
32. Smidt N, van der Windt DA, Assendelft WJ, et al. Corticosteroid injections, physiotherapy, or a wait and see policy for lateral epicondylitis: a randomised controlled trial. Lancet. 2002;359(9307):657–62.